



Experimental and numerical evaluation of compression confinement techniques for HSC beams reinforced with different ratios of high strength steel reinforcement

Abdo-Alfatah A. A. Graf

Faculty of Engineering, Zagazig University, Egypt

grafabdo2016@gmail.com, <https://orcid.org/0000-0002-6422-4252>

Mohamed Bneni

Faculty of Engineering, University of Zawia, Libya

Mohamedbneni@yahoo.com, <https://orcid.org/0000-0002-4352-5654>

Abd El-Monem I. El-Kholy, Ahmed. M. E. Elkilani, Seleem S. E. Ahmad

Faculty of Engineering, Zagazig University, Egypt

str.eng.elkholy@gmail.com, <https://orcid.org/0000-0003-4247-2041>

eng_3azab99@yahoo.com, <http://orcid.org/0000-0001-6188-205x>

seleemahmad62@yahoo.com, <http://orcid.org/0000-0001-9894-0209>

ABSTRACT. This work presents experimental and numerical research to evaluate the compression confinement techniques of HSC beams reinforced with different ratios of high-strength steel reinforcement. Twelve specimens of high-strength reinforced concrete beams with two different compression confinement techniques were tested experimentally. The first method is used carbon fiber reinforced polymers sheets (CFRPs) around the compression zone, CF, and the steel fibers reinforced concrete is used in the compression zone by 1% of volume fraction, SF, in the second case. A 3-D finite element analysis was done; using the ANSYS program to simulate and idealize all experimental specimens. The numerical and experimental results of the RC beams were validated and compared in this work. The results showed that there is a good idealization using 3-D finite element models with the experimental specimens. Also, it was found that using the suggested techniques can increase the strength ratio and increase the ductility index depending on the tensile reinforcement ratios. Moreover, the energy absorption and the mode of failure were enhanced.



Citation: Graf, A.-A. A. A., Bneni, M., El-Kholy, A. M. I., Elkilani, A. M. E., Ahmad, S. S. E., Experimental and numerical evaluation for compression confinement techniques of HSC beams reinforced with different ratios of high strength steel reinforcement, *Frattura ed Integrità Strutturale*, 60 (2022) 310-330.

Received: 21.12.2021

Accepted: 25.01.2022

Online first: 27.02.2022

Published: 01.04.2022

Copyright: © 2022 This is an open access article under the terms of the CC-BY 4.0, which permits unrestricted use, distribution, and reproduction in any medium, provided the original author and source are credited.

KEYWORDS. HSC beams; confinement techniques; ANSYS; Carbon fiber reinforced polymers; Steel fiber; Ductility; Mode of failure.



INTRODUCTION

High strength concrete is widely used in the present days because of the civilization revolution over the world. The high strength concrete has a dangerous brittle behavior and structural elements constructed using HSC usually fail in a brittle manner. The brittle behavior is not favorable condition, so the improvement of high strength concrete HSC behavior is very important. We can improve the failure by strengthening the compression zone with ductile materials by using additional compression steel reinforcement bars.

Using highly ductile fiber-reinforced concrete (HDC), characterized by its ability to absorb large ultimate strains, Mingke Deng et al. [1] investigated the effectiveness of HDC in improving deformational characteristics and the failure mode of over-reinforced concrete beams. Concrete beams that are over-reinforced often collapse suddenly due to compressive concrete crushing before the tensile steel reinforcement has yielded. In over-reinforced concrete beams with increased longitudinal reinforcement ratios and thick HDC layers, an increase in ductility of up to 61% can be achieved by adding HDC to the compression zone. By increasing the longitudinal reinforcement ratio, HDC became more effective at strengthening over-reinforced concrete beams.

Deesy Gomes Pinto et al.[2] studied the influence of high strength concrete beams confinement with stirrups reinforcement on the flexural ductility. In this study, the only variable is the reinforcement ratio of longitudinal tensile. The results showed a well positive effect on the flexural ductility due to confinement with stirrups reinforcement. The design ductility of high strength concrete columns and beams was studied in A.K.H. Kwan and J.C.M. Ho[3]. The results showed that the major factors that affect flexural ductility are the steel yield strength, concrete strength, confining pressure, and reinforcement ratio. Also, for columns the major factors affecting the flexural ductility were the steel yield strength, concrete strength, confining pressure, and axial load/stress level.

The effect of helically confinement of HSC beams on the displacement ductility was investigated by Muhammad N. S. Hadi and Nuri M. Elbasha[4] . In this work, ten over-reinforced HSC beams were tested. The results showed that the confinement effect is neglected for the helically confined beams when the pitch of the helical is equal to or more than the core diameter. Finally, this study shows that reduce helical pitch can enhance the strength and ductility of HSC beams reinforced with high strength reinforcement steel. Syed Wasim N Razvia and M. G. Shaikhb [5] studied the confinement effect on short concrete column behavior. The results indicated that column with additional confinement ferro mesh gives a 20% increase in axial load compared with regular control column. The results also approved that, columns with ferro mesh with additional stirrups gives better ductility moreover the column wrapped with ferro mesh only fails in ductile manner.

The flexural behavior of steel-reinforced, high-strength and prestressed concrete beams were experimentally investigated by Qing JIANG et al.[6] . The failure modes, ductility, flexural strength, and the specimen's crack width were analyzed. The results approved that the failure modes of high strength steel and high strength concrete prestressed beams were similar to the ordinary reinforced concrete. Mehrollah Rakhshani mehr et al. [7] studied experimentally the flexural ductility of RC beams with lap-spliced bars. The compressive strength of concrete, amount of stirrups over the splice length, and the longitudinal diameter bars were selected as the variables. The ductility of the specimens was evaluated based on the ductility ratio. Results showed that the previous variables have a major effect on the beams ductility. J. C. M. Ho et al. [8] investigated the minimum flexural design ductility of high strength concrete beams. Also, the maximum values of tension steel ratio and minimum curvature factor of ductility of the yield strengths steel and various concrete grades have been evaluated. The results concluded that to provide a level of minimum ductility, the minimum ductility factor should be 3·32.

22 beam tests were carried out by Jianwei Zhang et al. [9] to determine the bond behavior between reinforced concrete and recycled aggregate concrete (RAC). A significant increase in normalized peak bond strength is seen by increasing the concrete cover thickness and stirrup ratio. A positive correlation exists between RAC bond strength and $f_c^{1/2}$, which is similar to NAC bond strength and $f_c^{1/2}$.

The analytical and numerical approaches were proposed by Jorge Luis Palomino Tamayo and Gabriel Orso Garcia [10] to study the behavior of high strength reinforced concrete beams. Results of nineteen high strength reinforced concrete beams were compared with the proposed approach. It has been found that the model based on a constant ultimate strain at peak stress was acceptable to validate the numerical results with the experimental, so, some codes of practice suggest these parameters.

S.H. Chowdhury and Y.C. Loo [11] investigated the damping and cracking in high-strength reinforced concrete beams. Eight full-size high strength reinforced concrete, HSC, beams were tested experimentally. The average and maximum crack widths of all beams have been measured. Also, the beams were subjected to free vibration load. Two formulas were



developed to predict the average and maximum crack widths for reinforced concrete beams and the third formula for damping. Seleem S. E. Ahmad et al. [12] study the confinement effect on the behavior of over-reinforced high strength concrete beams. The testing results of all beams proved that the suggested techniques gave the behavior of a good beam, the first crack and ultimate loads of the beams were increased. Moreover, the mode of failures was changed from sudden failure for control beam to ductile failure for confinement beams.

In this work, experimental and numerical works for evaluation the compression confinement techniques of HSC beams reinforced with different ratios of high strength steel reinforcement. Two techniques were used, the first was using carbon fiber reinforced polymers (CFRPs) as confinement strengthening around the compression zone and the second technique was using additional steel fiber reinforced concrete in the half of the beam with a volume fraction equal to 1.0 %. Twelve high-strength reinforced concrete beams with two different compression confinement techniques were tested.

EXPERIMENTAL PROGRAM

Tab. 1 presents reinforced concrete beams that were fabricated and tested to investigate the behavior of high strength reinforced concrete beams with different compression confinement techniques, as shown in Fig. 1.a, b, and c. Fig. 2 shows cross section dimensions for control beams and steel bars reinforcement distribution where dimensions and steel bars diameter are in mm. The beams had been loaded up to failure using a load control machine.

Beam Code.	Description	Tensile Ast
C1	Control with ϱ_{\min}	2φ12mm
C2	Control with ϱ_{avg}	4φ16mm
C3	Control with ϱ_{\max}	7φ16mm
C4	Control with $\varrho > \varrho_{\max}$	8φ16mm
CF1	CFRPs confinement in compression zone with ϱ_{\min}	2φ12mm
CF2	CFRPs confinement in compression zone with ϱ_{avg}	4φ16mm
CF3	CFRPs confinement in compression zone with ϱ_{\max}	7φ16mm
CF4	CFRPs confinement in compression zone with $\varrho > \varrho_{\max}$	8φ16mm
SF1	Steel fiber 1.0% V_f in compression zone with ϱ_{\min}	2φ12mm
SF2	Steel fiber 1.0% V_f in compression zone with ϱ_{avg}	4φ16mm
SF3	Steel fiber 1.0% V_f in compression zone with ϱ_{\max}	7φ16mm
SF4	Steel fiber 1.0% V_f in compression zone with $\varrho > \varrho_{\max}$	8φ16mm

Table 1: Configurations of test specimens

The experimental work was divided into three groups according to the strengthening technique, the first group was for control beams without any strengthening, the second was for using one layer of carbon fiber reinforced polymers (CFRPs) sheets as a confinement reinforcement in the compression zone, and the third group was for using steel fiber reinforced concrete in compression zone with 1.0% volume fraction as confinement reinforcement.

MATERIAL PROPERTIES

The properties of the materials used concrete and steel were tested. A compression test, according to Egyptian Standard Specification, ESS, 1658-6/2018, and BS EN 12390/2009, was done for three cubic concrete samples during each beam casting; after 28-days all samples were tested as shown in Fig. 3. The average compressive strength value samples were equal to 65 MPa with STD equal to 2.51 MPa. A tension test, according to Egyptian Standard Specification,

ESS, 262-2/2015, and ISO 6935-2/2007, were done for the reinforcement steel bars as shown in Fig. 4. For each diameter, three samples were tested. The average results for main reinforcement steel and stirrup bars are given in Tab. 2.

Steel/Property.	Yield strength, MPa	Tensile strength, MPa	% Maximum of elongation
Main steel, Grade 550	550	700	15
Confinement steel, Grade 240	240	350	25

Table 2: Tension test results for main reinforcement steel and stirrup bars.

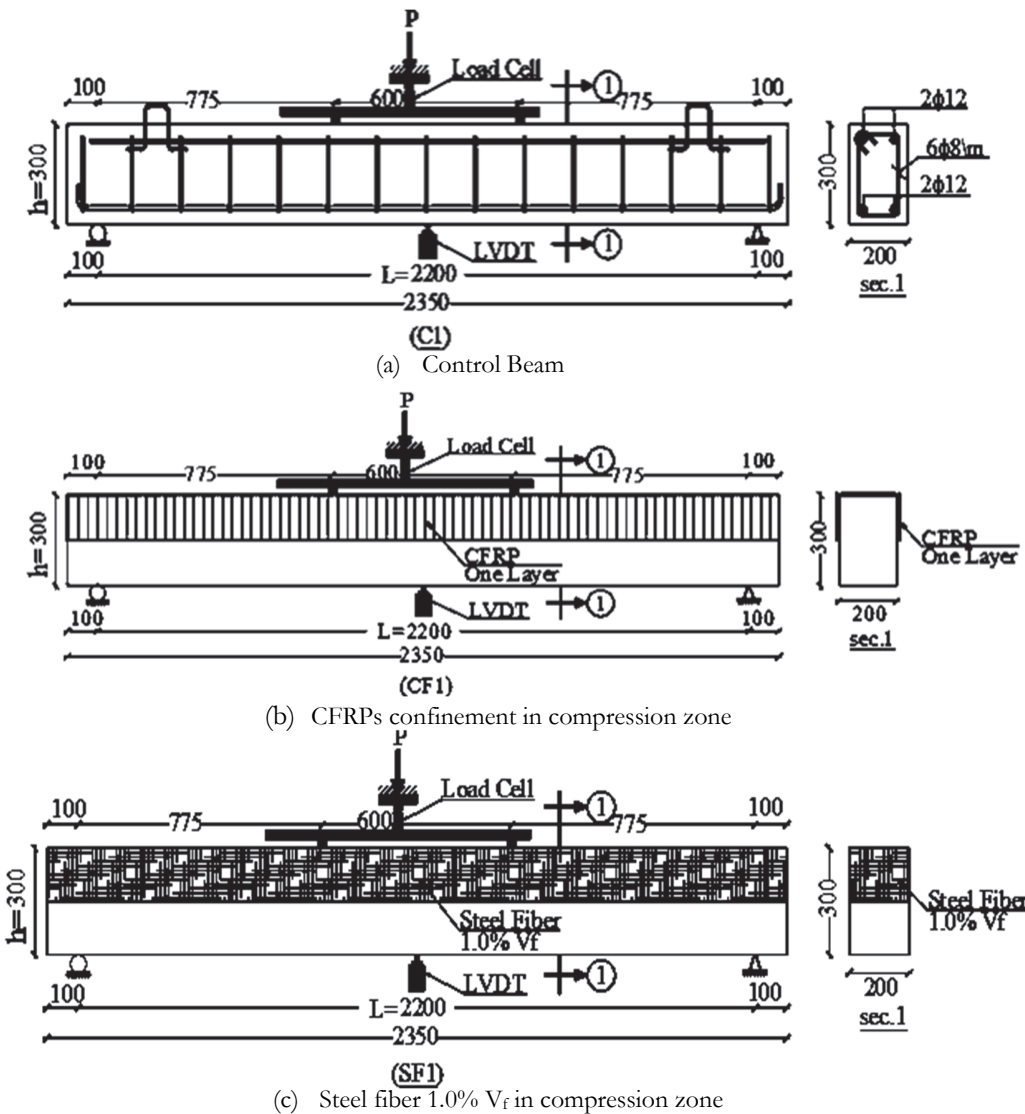


Figure 1: Experimental specimen schematics and dimensions; (a) control beams, (b) CFRPs confinement in compression zone and (c) steel fiber 1.0% V_f in compression zone.

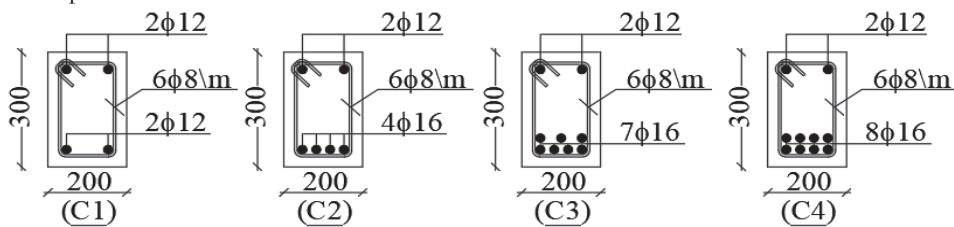


Figure 2: Cross section dimensions and steel bars distribution for control beams; C1, C2, C3, and C4.



Figure 3: Standard compression test for cube specimens.



Figure 4: Standard tension test for steel reinforcement.

The high elastic modulus, HM, CFRP fabric used to strengthen the specimens was unidirectional with nonstructural weaves in the transverse direction to hold the fabric together. According to the datasheet provided by the manufacturer, a dry fabric would have a tensile strength of 3.45 GPa, a high elastic modulus of 230 GPa, and elongation at a break of 1.5%, [13]. The fabric was laminated to the specimens with an epoxy resin having a tensile strength of 33.8 MPa and an ultimate elongation of 1.2%, according to Sikadur®-330 epoxy datasheet, [14].

TEST PROCEDURE

The beams were tested to failure by using a universal testing machine with 1000 KN capacity and 0.4% error of calibration while the rate of loading was 0.7 N/sqmm/min. Two rollers support were used for the beams. The load was applied in two points with a 600 mm distance between the two points, and the deflection was measured at the beam mid-span using linear vertical displacement transducers (LVDT) as shown in Fig. 5. All the beams were painted with white color to simplify the cracks observation, and the crack propagation was observed by the naked eye. A load control was used to test the samples, and the load-displacement values were recorded during loading using a data logger system.

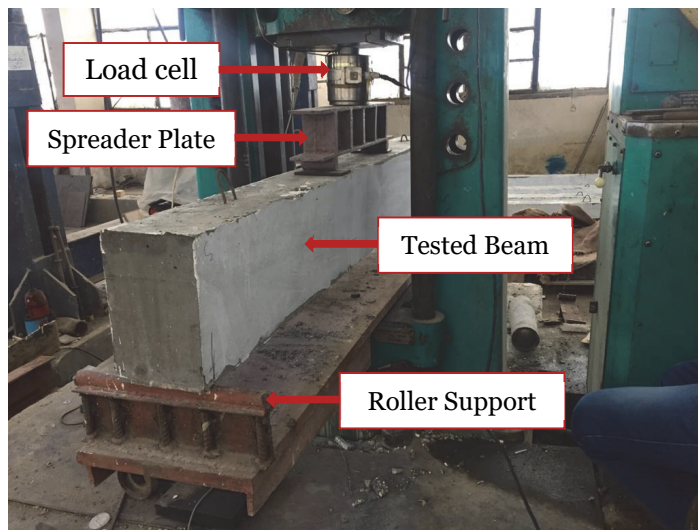


Figure 5: Test setup

NUMERICAL STUDY

A 3D finite element analysis (FEA) using ANSYS v2021 R1 was done to predict the behavior of high strength reinforced concrete beams confinement in compression zone with two techniques with different ratios of high strength steel reinforcement. The methodology of this work was done by building the 3D model, selecting the type of elements, the models of used materials, contact details, and selecting the type of analysis which considered the displacement control type.

Concrete was modeled using a suitable solid element for concrete properties named SOLID 65 with 8-nodes as shown in Fig. 6 a; reinforcement steel and steel fibers were modeled using REINF 264 element, while fiber reinforced polymers were modeled using SHELL 181 element shown in Fig. 6, b and SOLID 185 element was used to model the behavior of rigid the loading and bearing plates. In contrast, the bond slippage behavior between the FRPs sheets and the concrete was simulated using the cohesive zone model (CZM). The maximum shear contact stress was 3 MPa with a maximum debonding gap of 0.01 mm. In comparison, The maximum normal contact stress was 1 MPa with a maximum debonding gap of 0.01 mm [15]. Nonlinear analysis of the reinforced concrete beams was done based on the smeared crack approach with displacement control loading. The displacement load was applied to the top line of the loading plates, and the displacement convergence was included with tolerance value equal to 5%.

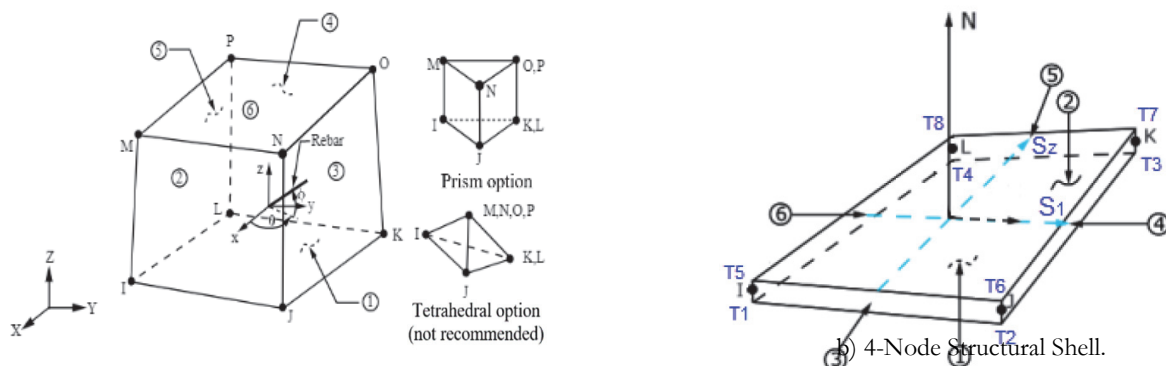


Figure 6: Elements used in modeling; a) SOLID65 concrete element b) 4-Node Structural Shell [13].



Concrete was simulated using a multilinear isotropic hardening model. The stress-strain curve was used to simulate the concrete plasticity based on equations 1 and 2 [16]. The concrete material properties are given in a Tab. 3.

$$f = \frac{E_c \varepsilon}{1 + \left(\frac{\varepsilon}{\varepsilon_0} \right)^2} \quad (1)$$

$$\varepsilon_0 = \frac{2f'_c}{E_c} \quad (2)$$

where, E_c is Young's modulus for concrete, ε is the concrete strain, and ε_0 is the compression failure strain.

Ultimate compressive strength	Tensile strength	Modulus of elasticity	Poisson's ratio
65 MPa	3 MPa	38 GPa	0.2

Table 3: Concrete material model properties

Uniaxial concrete tensile cracking stress was simulated according to the SOLID65 cracking model, as shown in Fig. 7.

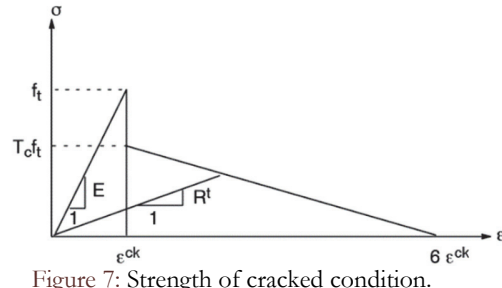
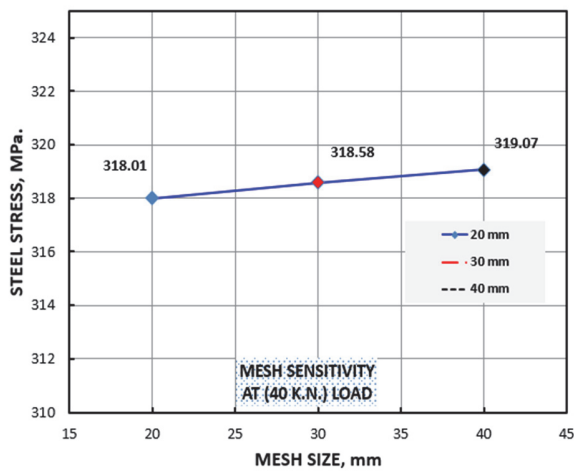
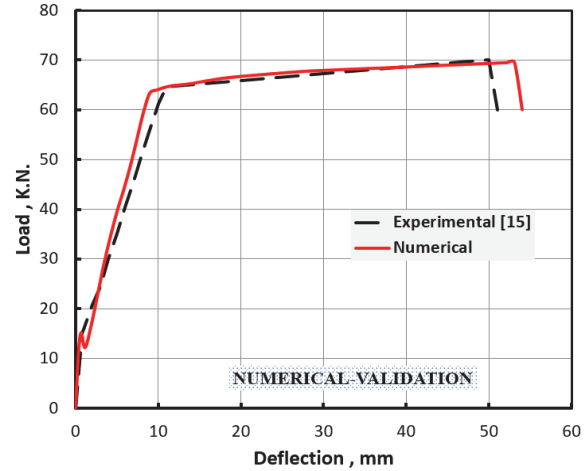


Figure 7: Strength of cracked condition.

The numerical model was validated by comparing the obtained numerical results for the control beam with the experimental data found in [17]. While sensitivity analysis was done by studying the element size effect 20, 30, and 40 mm on the steel stress results at 40 KN. The results in Fig. 8.a and Fig. 8.b show that the developed numerical model is acceptable for simulating the problem and the mesh element sizes 20, 30, and 40 mm have the same results, therefore, 25 mm element size was selected to model all beams.



a) Element mesh size sensitivity.



b) Numerical validation.

Figure 8: Results validation; a) Element mesh size sensitivity, b) Numerical validation.

The geometry of the experimental specimens was idealized and simulated numerically with the strengthening techniques as shown in Fig. 9.

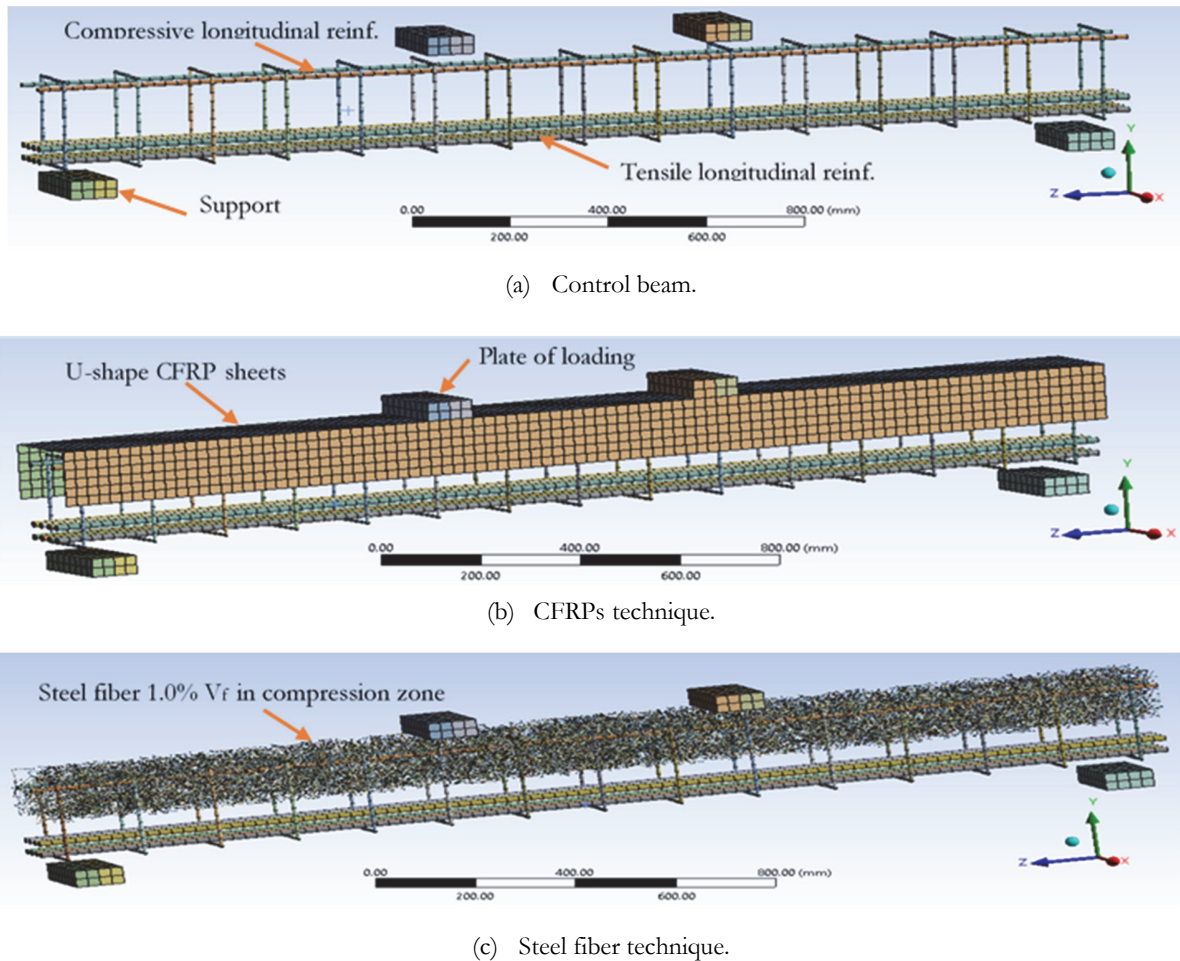


Figure 9: Finite Element Modeling; (a) Control beam, (b) CFRPs technique, and (c) Steel fiber technique.

RESULTS AND DISCUSSION

The experimental and numerical results of the strengthened high strength concrete beams (HSCB) were compared with the control beams results. The comparison includes the yield load, deflection, ultimate load, deflection, ductility index, and failure mode.

Experimental Results

Tab. 4, shows the comparison between the experimental results for control, C, carbon fiber reinforced polymers, CF, and steel fiber reinforced concrete, SF, beams at four steel reinforcement ratios ρ_{\min} , ρ_{avg} , ρ_{\max} , and $\rho > \rho_{\max}$.

Fig. 10 shows the experimental relationship between the applied load and mid-span deflection for control beam, C1, CFRPs, CF1, and steel fiber, SF1, techniques at steel reinforcement ratio equals ρ_{\min} . The results indicated that there is a linear behavior up to the first cracking load. The values of the first cracking load were recorded to equal 48.13, 57.89 and 100.3 KN for C1, CF1 and SF1 respectively. These results approved the positive effect of the used confinement techniques especially for the steel fiber reinforced confinement technique; where the cracking load value was increased from 48.13 KN for C1 to reach 100.3 KN for SF1 with an increasing percent of about 108.4%. This finding may be due to enhancing compression resistance of the upper part of the beam section as a result of confinement techniques. After that, the load-deflection curve exhibits non-linear behavior until it reaches the maximum point of load and deflection.



Similar behavior was reported for the values of ultimate load, P_u for the tested beams. The results show that the strengthening techniques can increase the ultimate load by about 23.80 and 52.73 % for CF1 and SF1 respectively. Moreover, for the CFRP confinement technique the values of cracking deflection, Δ_{cr} , and maximum deflection, Δ_u , were decreased as compared to the corresponding values control beam, C1. On the other hand, for steel fiber confinement technique, the values of cracking deflection, Δ_{cr} , and maximum deflection, Δ_u , were increased as compared to the corresponding values control beam, C1. The obtained results were approved a highly efficient technique for steel fiber confinement in increasing of ductility and strength of RC beams reinforced with ρ_{min} .

Beam code	P_{cr} (kN)	Δ_{cr} (mm)	P_u (kN)	Δ_u (mm)	μ	Failure mode
C1	48.13	3.43	89.70	76.18	22.21	CC
C2	255	15	257.75	17.90	1.193	SF
C3	324	18	324.54	21.00	1.16	SF
C4	313.66	17.53	315.66	23.00	1.31	SF
CF1	57.89	3.09	111.05	44.05	14.26	CC
CF2	257	17	258.42	20.38	1.198	SF
CF3	347	18	347.81	19.91	1.106	SF
CF4	346	22	346.18	28.47	1.294	SF
SF1	100.30	7.96	137.00	82.04	10.31	CC
SF2	297.42	16.07	338.46	47.32	2.94	CC
SF3	451.88	22.35	482.28	56.70	2.54	SF
SF4	500	27	516.99	30.11	1.115	SF

Table 4: Experimental results and failure modes of the tested specimens (where, P_{cr} = First crack load, Δ_{cr} = first crack deflection, P_u = ultimate load, Δ_u = maximum deflection, μ = ductility index, CC = concrete crushing, and SF = shear failure).

Figs. 11 a, b and c show cracks pattern and failure modes for beams C1, CF1 and SF1 respectively. All beams failed initially due to tension cracks followed by concrete compression failure. The cracks in beam C1 seemed to be less in number and wider as compared to other beams. While CF1 beam showed a debonding failure of CFRP and SF1 beam showed more in number and narrow cracks patterns in tension zone as compared to beam C1.

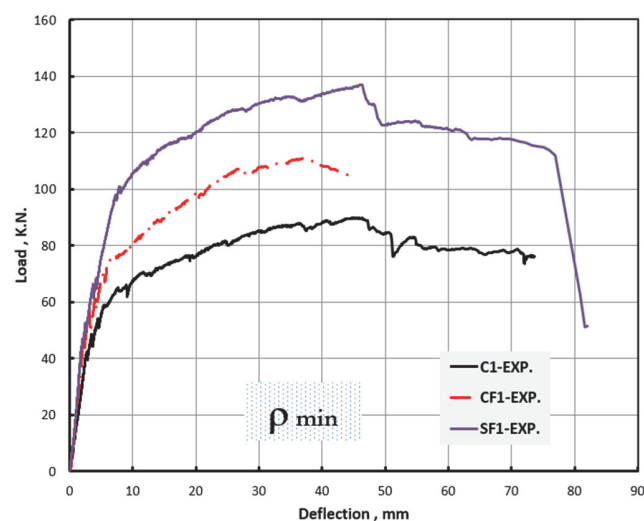


Figure 10: Experimental load-deflection relationship for C1, CF1 and SF1 techniques at ρ_{min} .

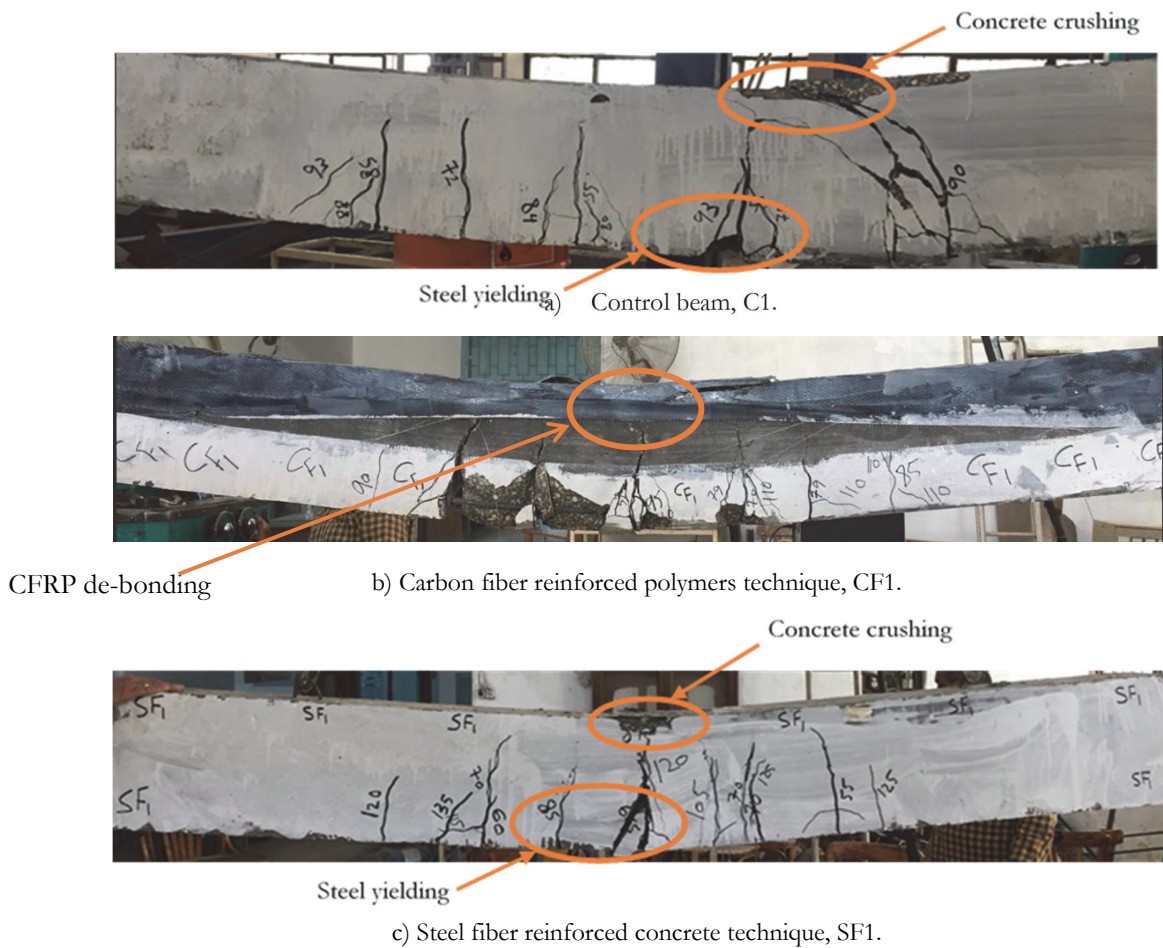


Figure 11: Crack patterns at maximum deflection; a) Control beam (C1), b) Carbon fiber reinforced polymers technique (CF1), and c) Steel fiber reinforced concrete technique (SF1).

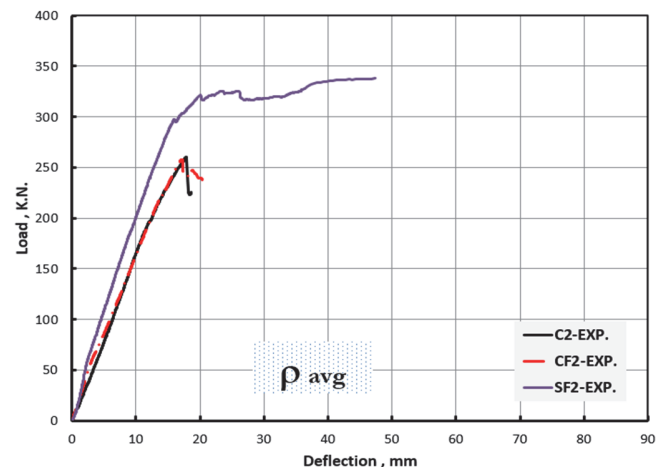


Figure 12: Experimental load-deflection relationship C2, CF2 and SF2 techniques at ρ_{avg} .

Experimental relationships between load and mid-span deflection for C2, CF2 and SF2 techniques at steel reinforcement ratio equal to ρ_{avg} are given in Fig. 12. Beams C2 and CF2 showed typical linear behavior of load-deflection response with approximately absent of nonlinear regime, the maximum loads value, P_u , are 257.75 kN and 258.42 kN respectively. On the other hand, beam SF2 exhibited a linear and nonlinear response with P_{cr} and P_u values of 297.42 kN and 338.46



kN respectively. The results, also, showed that the strengthening techniques increase the ultimate load about 0.26, and 31.31 % for CF2 and SF2 respectively. These results approved the positive effect of the steel fiber reinforced confinement technique as compared to CFRP technique. While Fig. 13 a, b, and c show crack pattern for RC beams using steel reinforcement equal to ρ_{avg} . All beams failed initially due to tension cracks followed by shear failure.

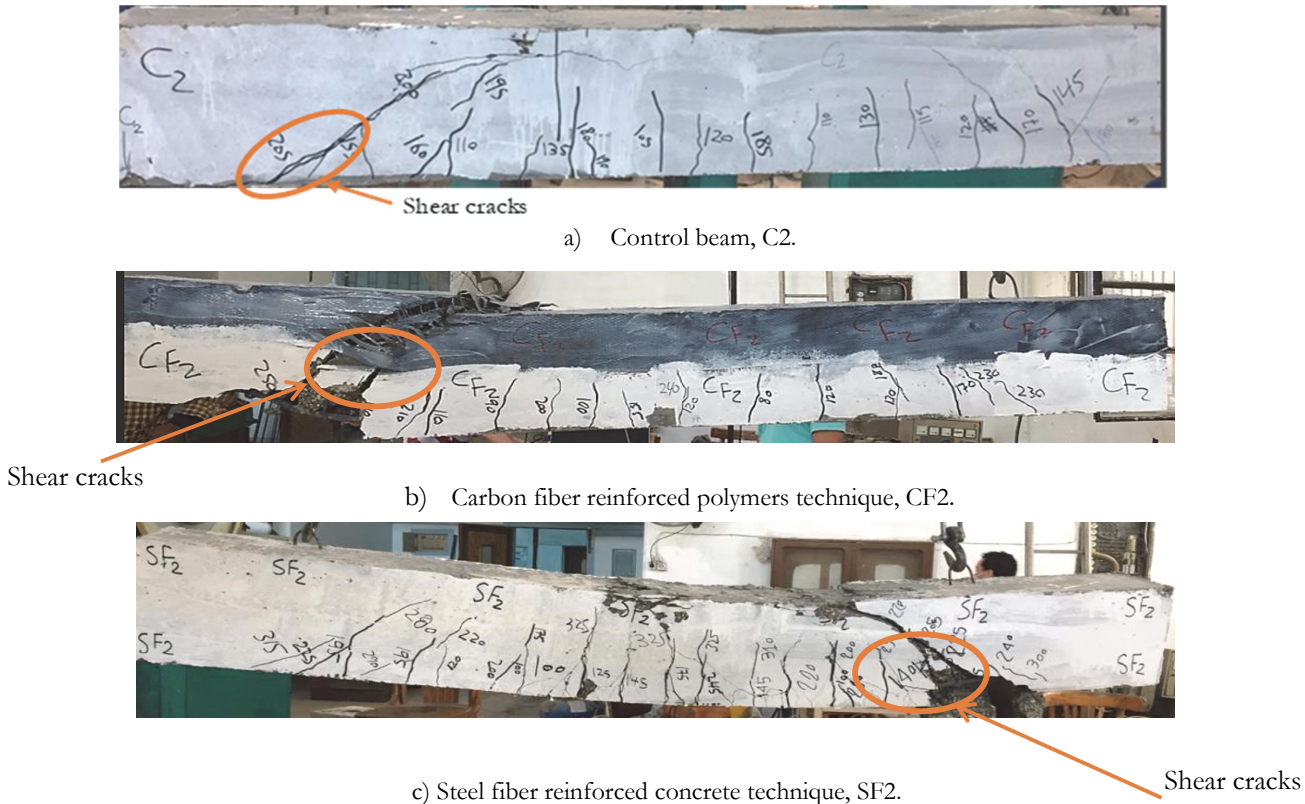


Figure 13: The crack patterns; a) Control beam (C2), b) Carbon fiber reinforced polymers technique (CF2), and c) Steel fiber reinforced concrete technique (SF2).

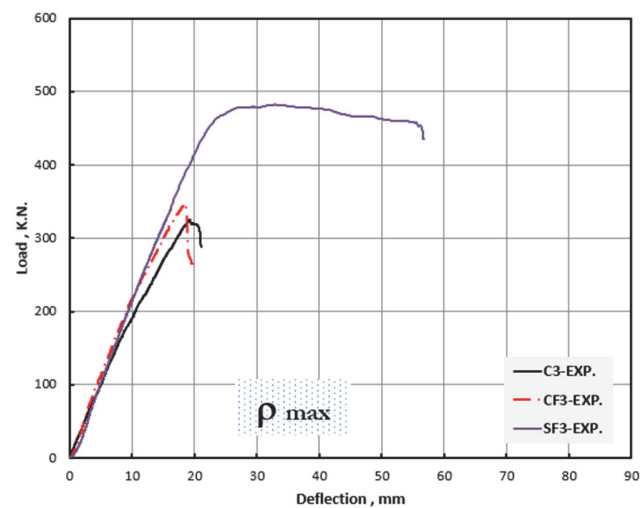


Figure 14: Experimental load-deflection relationship for control beam C3, CF3 and SF3 techniques using ρ_{max} .

Fig. 14 gives experimental relationships between load and mid-span deflection for C3, CF3 and SF3 techniques at steel reinforcement ratio equal to ρ_{max} . Beams C3 and CF3 showed typical linear behavior of load-deflection response with approximately absent of nonlinear regime, the maximum loads value, P_u , are 324.54 kN and 347.81 kN respectively. On

the other hand, beam SF3 exhibited a linear and nonlinear response with P_{cr} and P_u values of 451.88 kN and 482.8 kN respectively. The results, also, showed that the strengthening techniques increase the ultimate load by about 7.2 and 48.7 % for CF3 and SF3 respectively as compared to C3. These results clearly indicate that the CFRP confinement technique and steel fiber confinement technique are more effective at ρ_{max} . Moreover the obtained results, also, approved the positive effect of the steel fiber reinforced confinement technique as compared to CFRP technique. With respect to ductility behavior one can notice that for steel fiber, confinement technique the values of cracking deflection, Δ_{cr} , and maximum deflection, Δ_u , were increased as compared to the corresponding values control beam, C3 and CF3.

Fig. 15 a, b, and c show crack pattern for RC beams using steel reinforcement equal to ρ_{max} . All beams failed initially due to tension cracks followed by shear cracks up to complete failure.

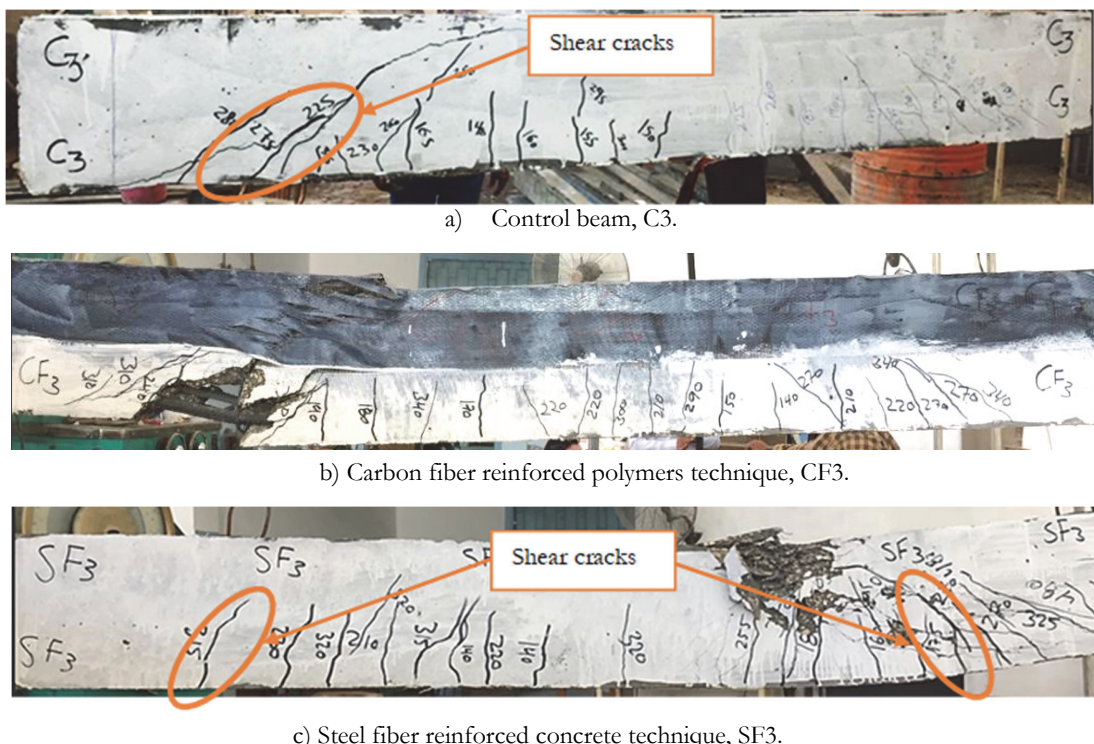


Figure 15: The crack patterns; a) Control beam (C3), b) Carbon fiber reinforced polymers technique (CF3), and c) Steel fiber reinforced concrete technique (SF3).

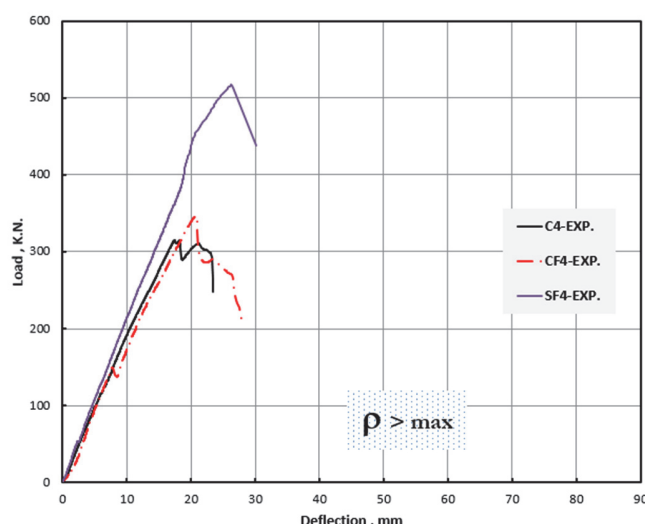


Figure 16: Experimental load-deflection relationship for control beam C4, CF4 and SF4 techniques using $\rho > \rho_{max}$.



The results of load and deflection for C4, CF4 and SF4 techniques at steel reinforcement equal to $\rho > \rho_{\max}$ are given in Fig. 16. The results indicated that there are similar behaviors as found in Fig. 12 for steel reinforcement ratio equal to ρ_{\max} . The maximum loads for beams C4 and CF4 were slightly decreased as compared to C3 and CF3 although increasing in steel reinforcement ratio. This behavior can be attributed to the shear failure generated in those beams. On the other hand, using steel fiber confinement technique in compression zone, beam SF4, improves the maximum load of SF4 as compared to SF3. Fig. 17 a, b, and c show crack pattern for RC beams using steel reinforcement equal to $\rho > \rho_{\max}$. All beams failed initially due to tension cracks followed by shear cracks up to complete failure.



a) Control beam, C4.

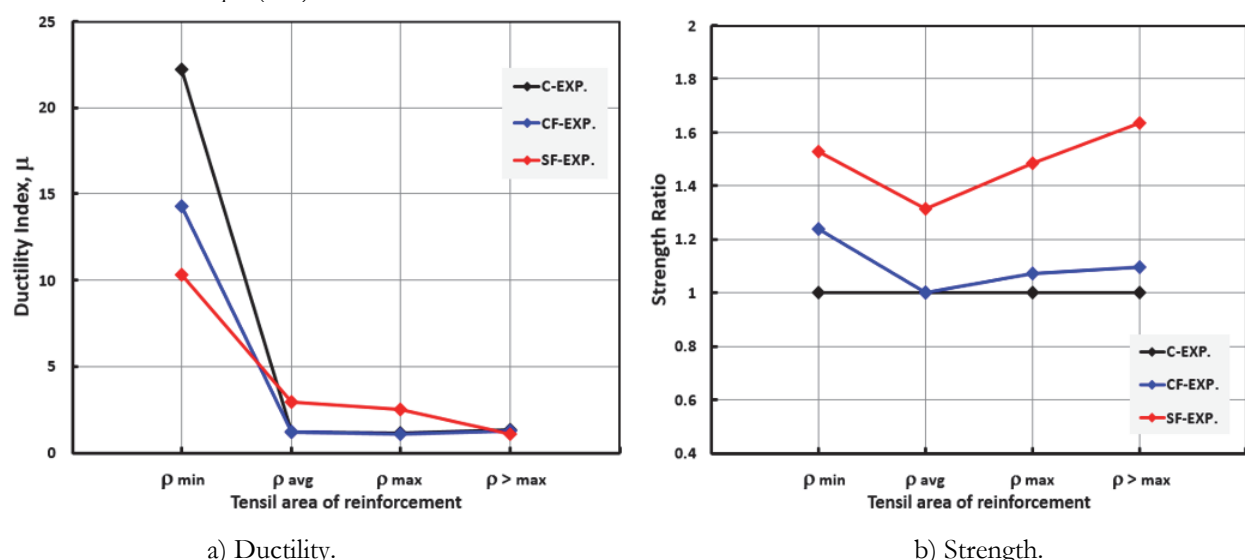


b) Carbon fiber reinforced polymers technique, CF4.



c) Steel fiber reinforced concrete technique, SF4.

Figure 17: The crack patterns; a) Control beam (C4), b) Carbon fiber reinforced polymers technique (CF4), and c) Steel fiber reinforced concrete technique (SF4).



a) Ductility.

b) Strength.

Figure 18: Effect of confinement techniques on; a) Ductility and b) Strength.

Fig. 18 a) and b) show the behavior of ductility index and strength ratio with the increase in steel reinforcement ratio for control beams and confinement beams. The ductility index was calculated as the ratio between maximum deflections to the first cracking deflection. The strength ratio was calculated as the ratio between maximum loads to first cracking load. From data in figures we found that, at ρ_{\min} , the CFRP confinement technique encases the ductility index more than steel fiber confinement technique. While at ρ_{avg} and ρ_{max} the steel fiber confinement technique gives more ductility than CFRP technique. On the other hand, the used confinement techniques were improved the strength ratio at all steel reinforcement ratios with obviously increasing in case of steel fiber.

NUMERICAL RESULTS

Tab. 5 shows numerical results of 3-D FE models in this work for control models, C, carbon fiber reinforced polymers, CF, and steel fiber reinforced concrete, SF at four steel reinforcement ratios ρ_{\min} , ρ_{avg} , ρ_{max} , and $\rho > \rho_{max}$.

Beam code.	P _{cr} (kN)	Δy (mm)	P _u (kN)	Δu (mm)	μ	Failure mode
C1	60.98	5.55	88.34	74.40	13.41	CC
C2	200.93	7.44	243.91	33.91	4.56	CC
C3	301.41	9.11	349.97	20.65	2.27	CC
C4	339.90	9.77	385.28	18.99	1.94	CC
CF1	61.50	5.89	89.94	50.12	8.51	CC
CF2	203.48	7.77	255.27	32.00	4.12	CC
CF3	304.27	9.28	353.95	14.46	1.56	CC
CF4	338.61	9.78	388.42	15.25	1.56	CC
SF1	63.82	5.54	104.14	72.25	13.04	CC
SF2	202.66	7.44	262.03	55.42	7.45	CC
SF3	322.96	9.80	359.39	33.33	3.40	CC
SF4	345.66	9.78	392.30	22.61	2.31	CC

Table 5: Numerical results of the FE Models. where, P_y and Δy = yielding load and deflection, P_u = ultimate load, Δu = maximum deflection, μ = ductility index, CC = concrete crushing, and SF = shear failure.

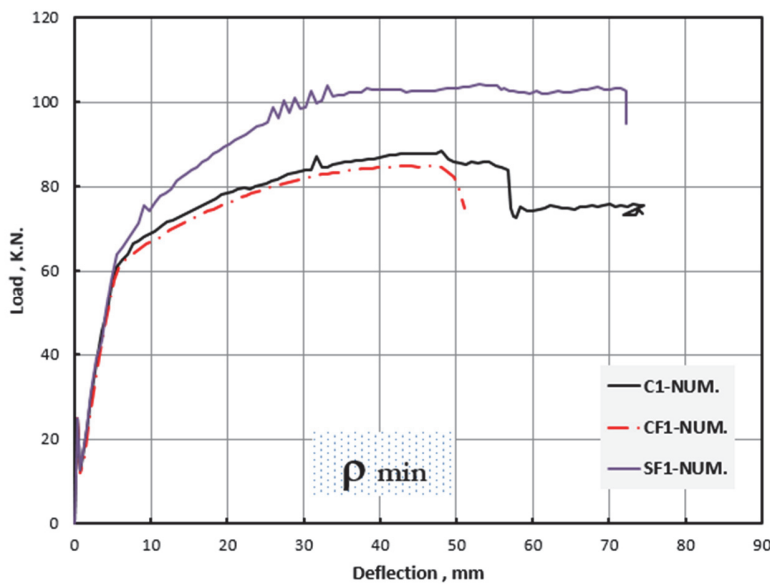


Figure 19: Numerical load-deflection relationship for C1, CF1, and SF1 techniques at ρ_{\min} .



Fig. 19 shows the numerical relationship between applied load and mid span deflection for C1, CF1 and SF1 beams at steel reinforcement ratio equals to ρ_{min} . The numerical results showed that similar behaviors as found in experimental results. The behavior started with linear response up to cracking load, P_{cr} , and followed by nonlinear response up to the values of maximum load, P_u , and deflection, Δ_u . Moreover, SF1 beam showed higher values of P_{cr} and P_u as compared to C1 and CF1 beams. This behavior can attribute to the effect of steel fiber confinement which prevents the early compression failure and lets the steel reinforcement carry additional loads. The numerical failure modes of these beams are given in Fig. 20 a, b and c. All beams showed tensile cracks followed by crushing in compression zone. Beam CF1 showed, also, de-bonding failure for CFRP sheets.

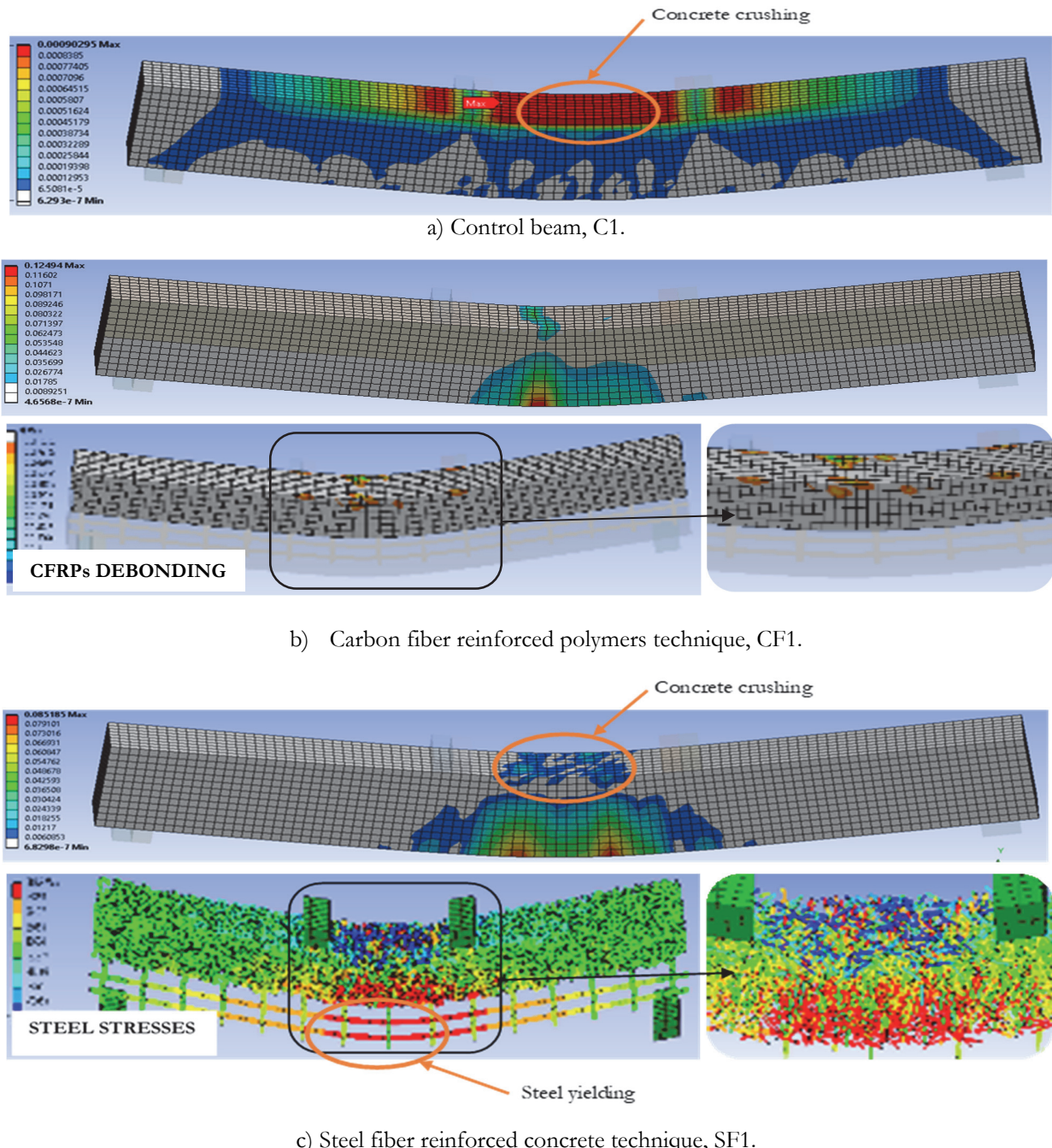


Figure 20: The crack patterns; a) Control beam (C1), b) Carbon fiber reinforced polymers technique (CF1), and c) Steel fiber reinforced concrete technique (SF1).

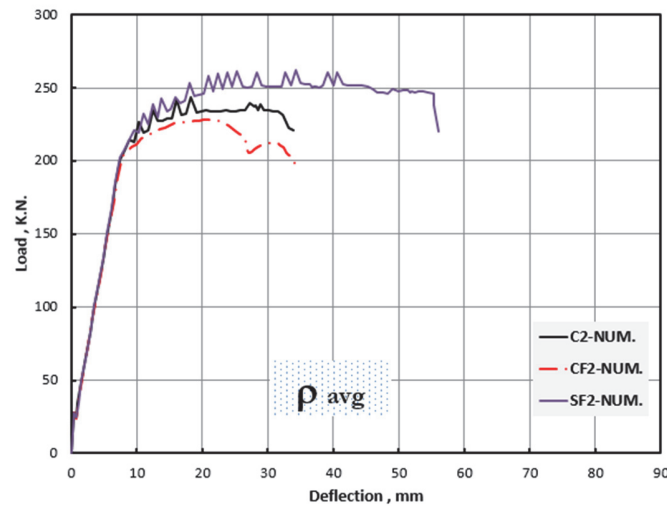
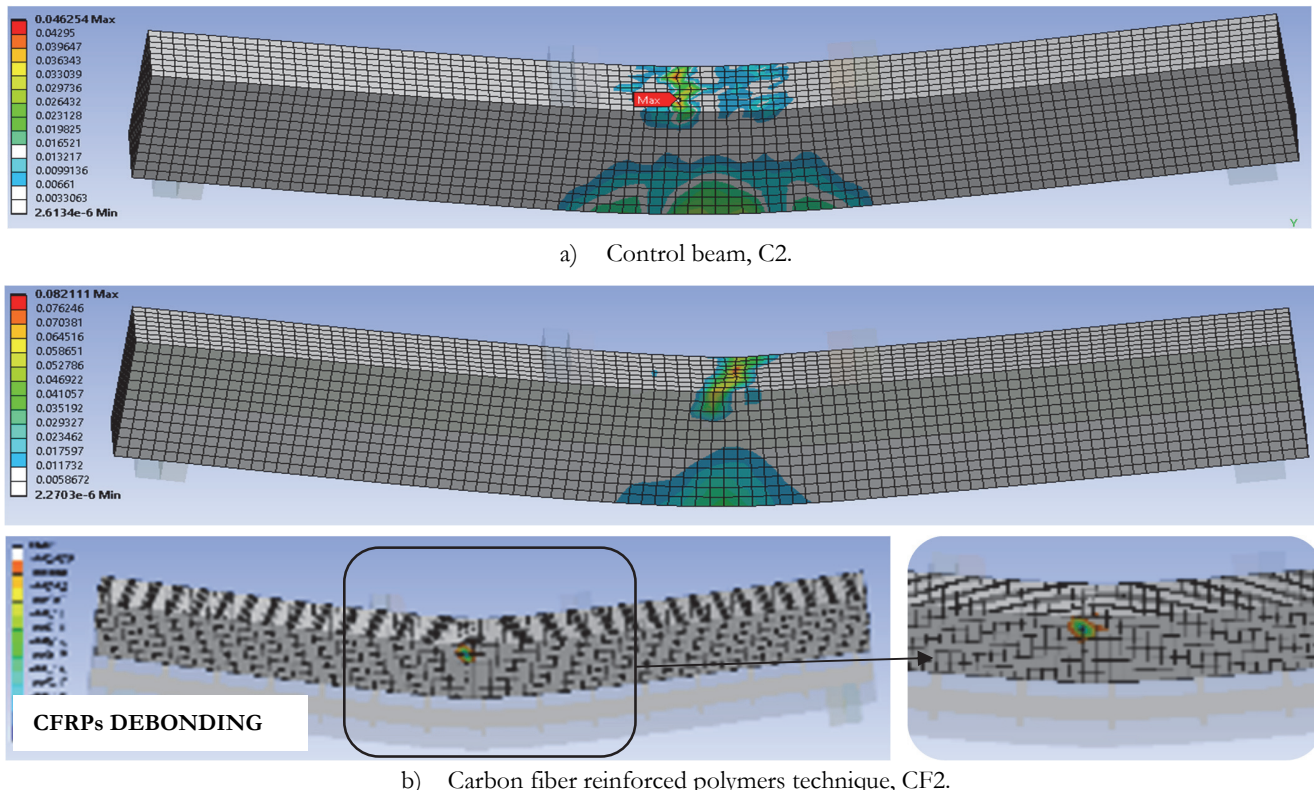
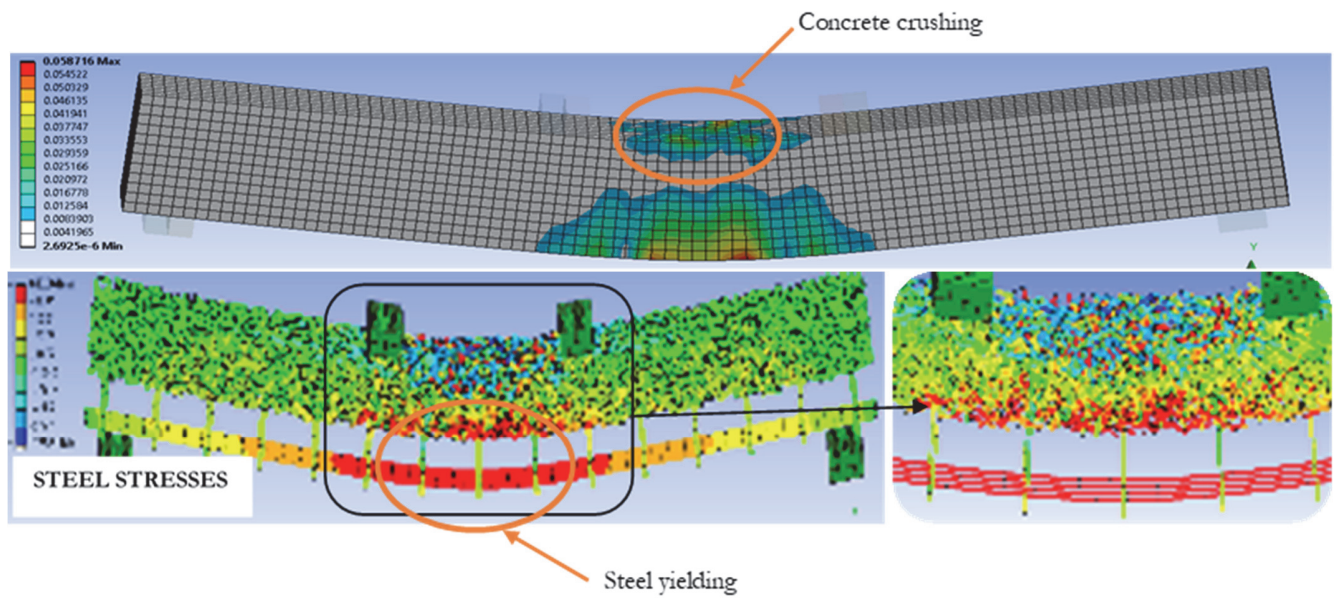


Figure 21: Numerical load-deflection relationship for C2, CF2 and SF2 techniques at ρ_{avg} .

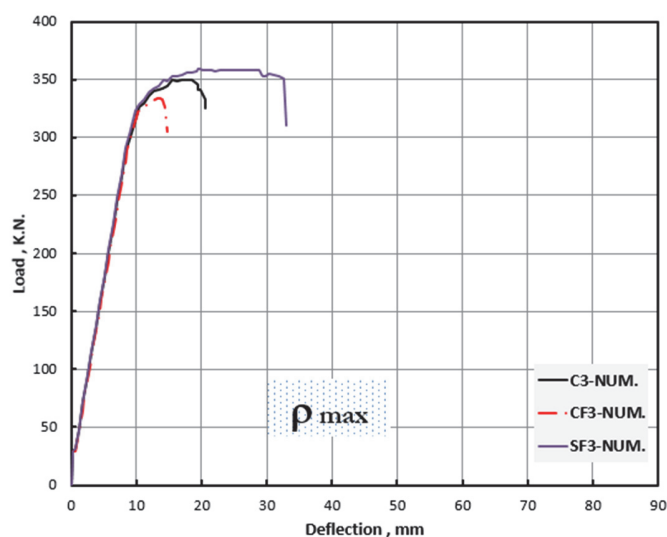
The numerical results of load-mid span deflection for C2, Cf2 and SF2 beams are presented in Fig. 21 at ρ_{avg} . Typical behaviors of linear and nonlinear response were found as in case of ρ_{min} with an increase in the value of P_{cr} and P_u as compared to ρ_{min} due to increase in the ratio of steel reinforcement. On the other hand, the values of cracking and maximum deflection were decreased as compared to those of ρ_{min} . Fig. 22 a, b and c show crack pattern for beams at steel reinforcement equal to ρ_{avg} .





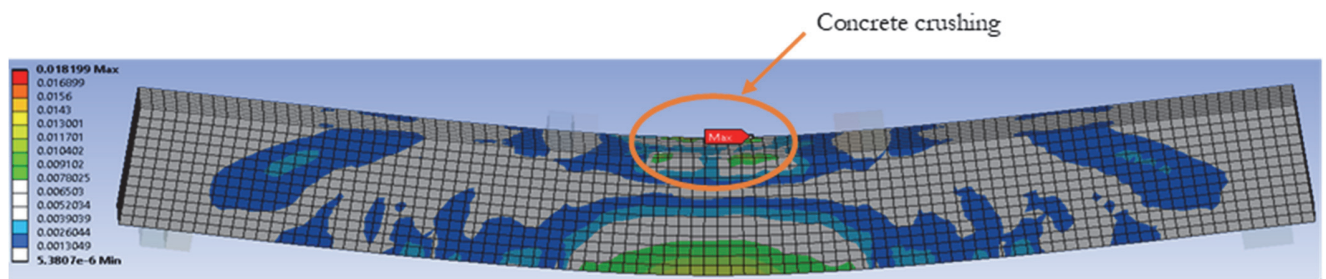
c) Steel fiber reinforced concrete technique, SF2.

Figure 22: The crack patterns; a) Control beam (C2), b) Carbon fiber reinforced polymers technique (CF2), and c) Steel fiber reinforced concrete technique (SF2).

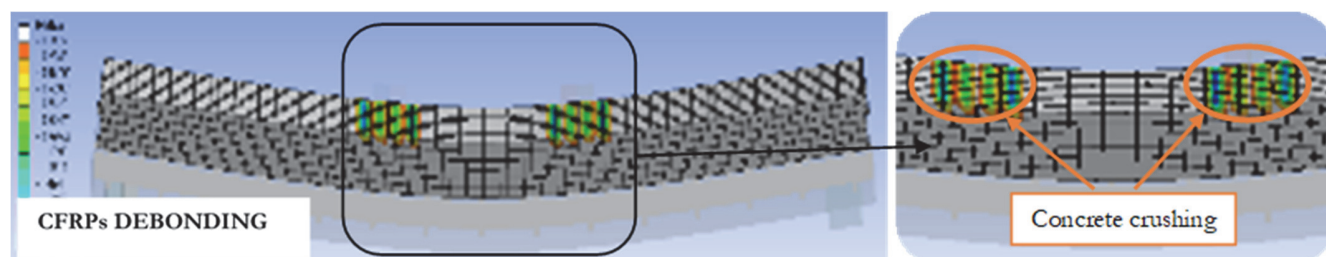
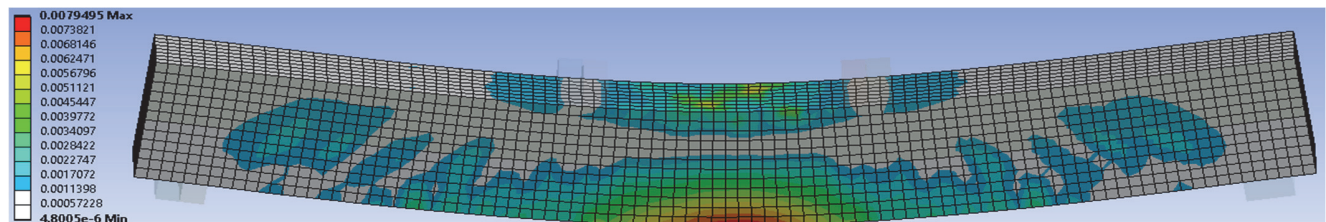
Figure 23: Numerical load-deflection relationship for C3, CF3 and SF3 techniques at ρ_{\max} .

As the ratio of steel reinforcement increases, beams of ρ_{\max} and $\rho > \rho_{\max}$, typical numerical behavior for load-deflection was reported as shown in Figs. 23 and 25 respectively. The cracking and maximum load of two beams were going to increase and deflection decreases. The numerical modes of failure for the beams of ρ_{\max} and $\rho > \rho_{\max}$ are given, also, in Figs. 24 and 26 respectively. All beams showed tensile cracks followed by crushing in compression zone.

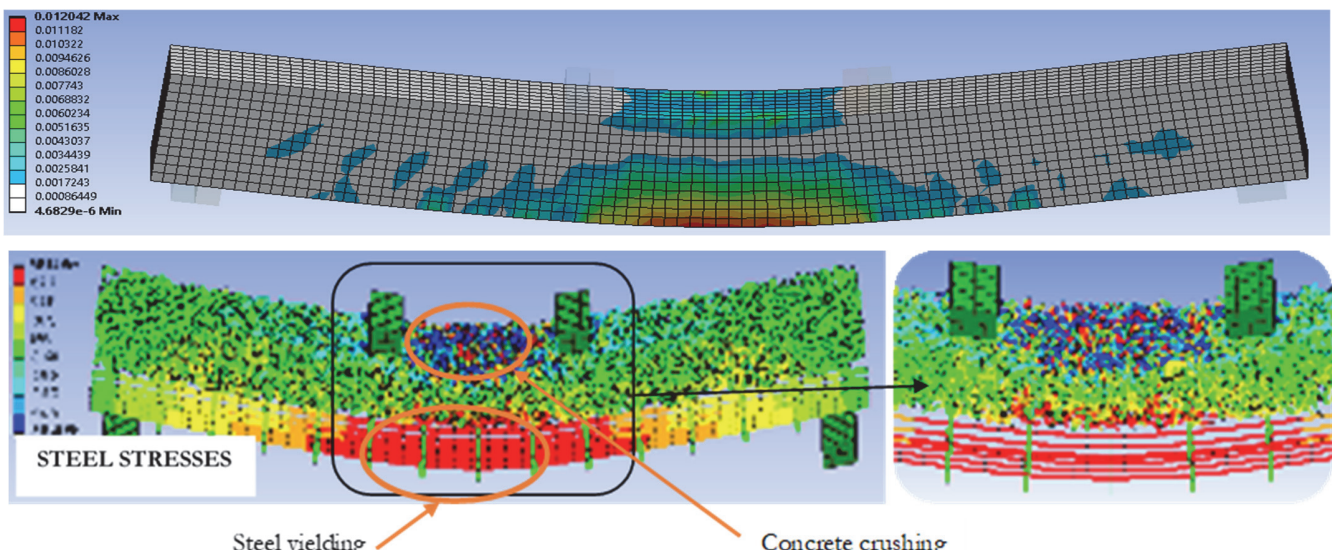
Fig. 27 shows the numerical behavior of ductility index and strength ratio with the increase in steel reinforcement ratio for control beams and confinement beams. The ductility index was calculated as the ratio between maximum deflections to the first cracking deflection. The strength ratio was calculated as the ratio between maximum loads to first cracking load. From data in figures we found that, at ρ_{\min} , ρ_{avg} and ρ_{\max} the steel fiber confinement technique gives more ductility than CFRP technique. Moreover, the SF confinement technique was improved the strength ratio at all steel reinforcement ratios with slightly decreasing in case of CFRP.



a) Control beam, C3.



b) Carbon fiber reinforced polymers technique, CF3.



c) Steel fiber reinforced concrete technique, SF3.

Figure 24: The crack patterns; a) Control beam (C3), b) Carbon fiber reinforced polymers technique (CF3), and c) Steel fiber reinforced concrete technique (SF3).

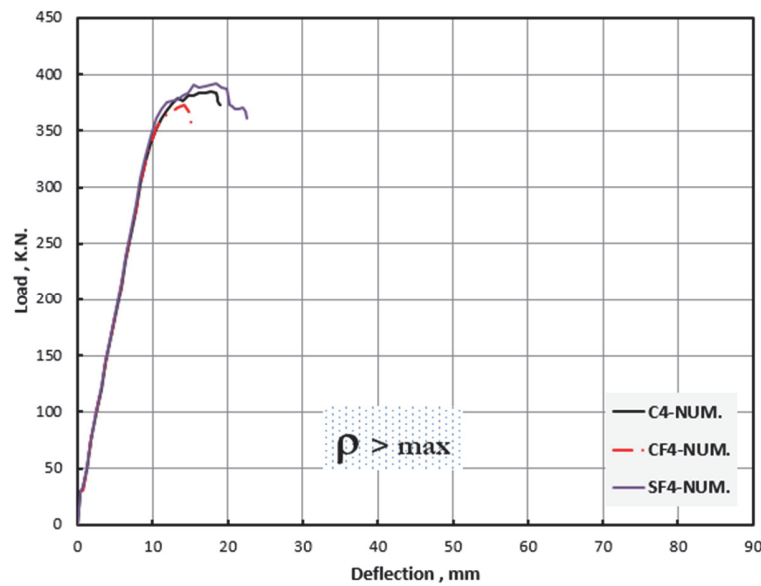
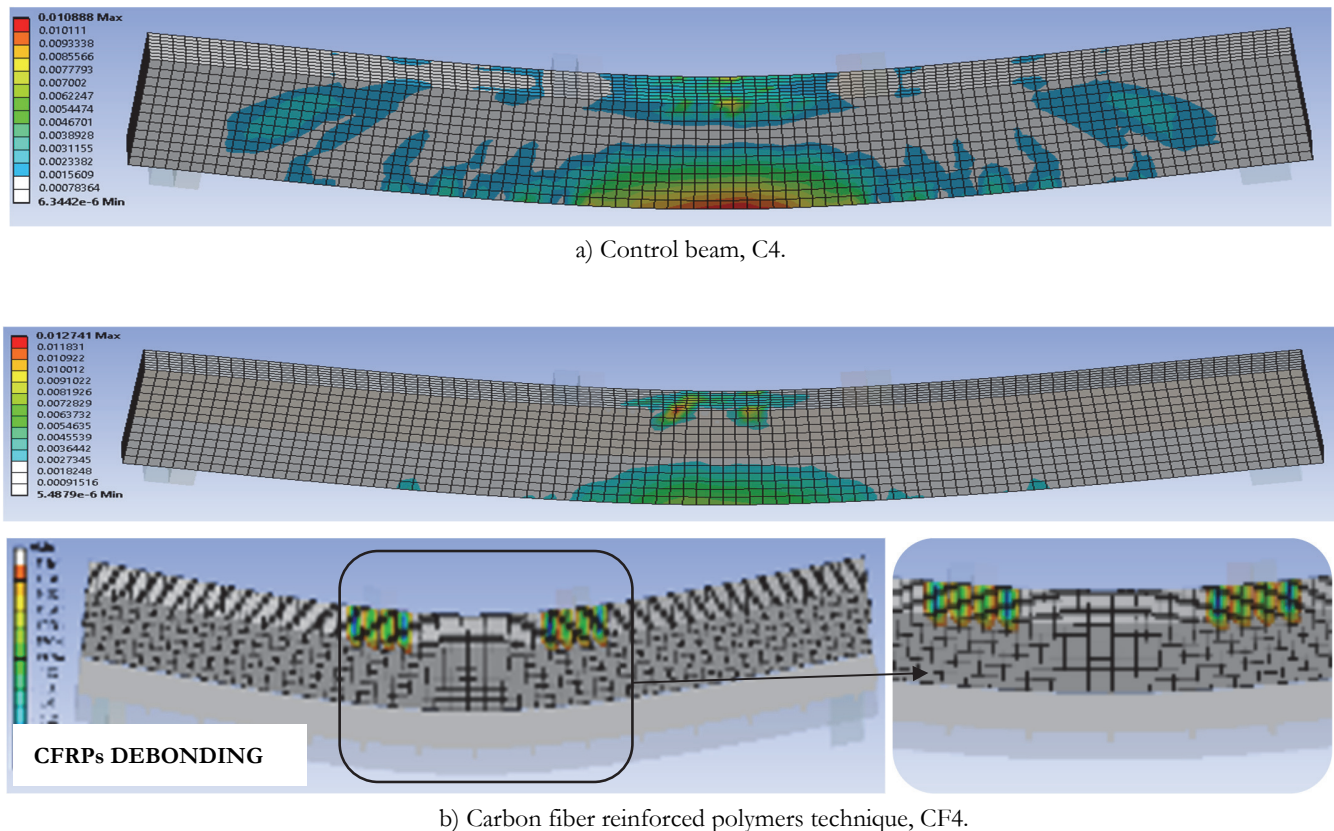
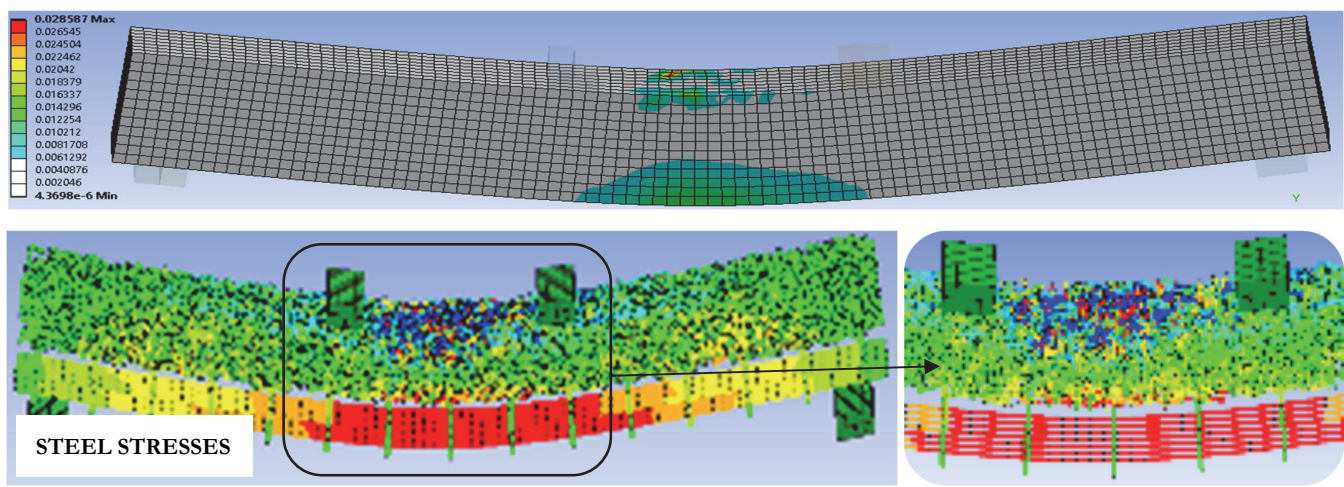


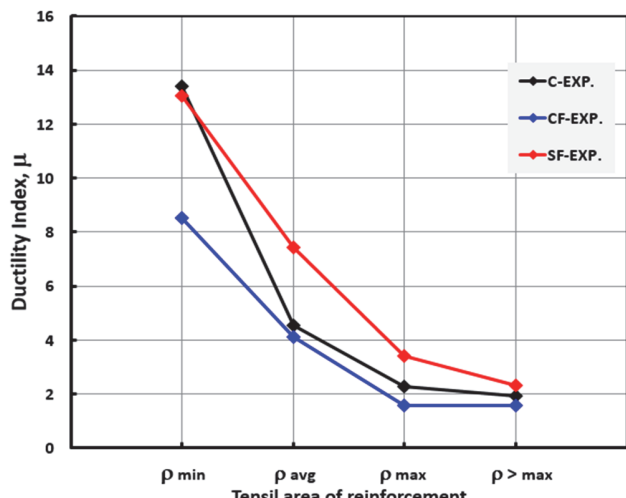
Figure 25: Numerical load-deflection relationship for C4, CF4 and SF4 techniques at $\rho > \max$.



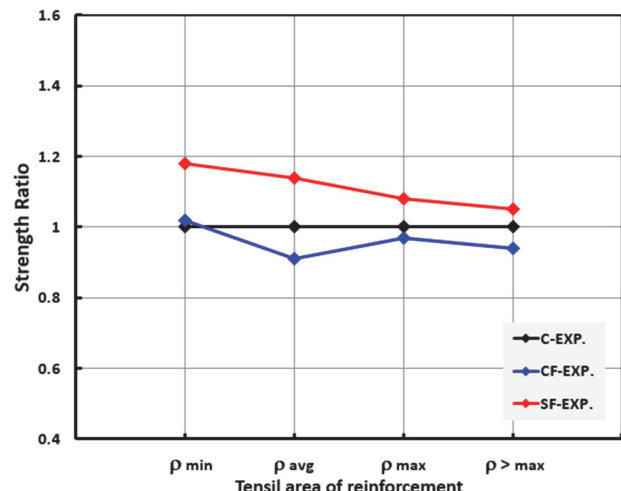


c) Steel fiber reinforced concrete technique, SF4.

Figure 26: The crack patterns; a) Control beam (C4), b) Carbon fiber reinforced polymers technique (CF4), and c) Steel fiber reinforced concrete technique (SF4).



a) Ductility.



b) Strength.

Figure 27: Effect of confinement techniques on; a) Ductility, b) Strength.

CONCLUSIONS

An experimental and numerical study was conducted, including testing and simulating twelve samples of high strength reinforced concrete beams with different compression confinement techniques. The following conclusions can be written from this study:

- 1- For steel fiber reinforced confinement technique the cracking load value was improved by about 108.4% and the maximum load was improved by about 52.73 % at minimum area of steel reinforcement.
- 2- The steel fiber strengthening techniques increases the ultimate load by about 48.7 % at average area of steel reinforcement.
- 3- For maximum steel reinforcement ratios, using the steel fiber reinforced technique can increase the strength and ductility ratios by 8% and 118% respectively.
- 4- Using carbon fiber reinforced polymers technique has a slight effect on the strength and ductility index.



- 5- For steel reinforcement ratios more than the maximum ratios, using the steel fiber reinforced technique can increase the strength and ductility ratios by 5% and 48% respectively.
- 6- The numerical results and experimental results in this work were not identical in values but they showed that similar behaviors as found in the results of ductility index and strength ratio with the tensile area of steel reinforcement ratio.

REFERENCES

- [1] Deng, M., Zhang, M., Ma, F., Li, F., Sun, H. (2021). Flexural strengthening of over-reinforced concrete beams with highly ductile fiber-reinforced concrete layer, *Engineering Structures*, 231, 111725.
- [2] Pinto, D. G., Bernardo, L. F. A. and de Oliveira, L. A. P. (2006). Influence of Confinement with Transverse Reinforcement on the Flexural Ductility of High-Strength Concrete Beams. Inocs 06, International Conference on Concrete for Structures, Rio de Janeiro, Brazil.
- [3] Kwan, A. and Ho, J. (2010). Ductility design of high-strength concrete beams and columns," *Advances in Structural Engineering*, 14(4), pp. 651-664.
- [4] Hadi, M. N. and Elbasha, N. (2008). Displacement ductility of helically confined HSC beams. *The Open Construction and Building Technology Journal*, 2, pp. 270-279.
- [5] Razvi, S. W. N. and Shaikh, M. ,(2018). Effect of confinement on the behavior of short concrete column, *Procedia Manufacturing*, 20, pp. 563-570.
- [6] Jiang, Q., Wang, H., Chong X. (2021). Flexural behavior of high-strength, steel-reinforced, and prestressed concrete beams, *Frontiers of Structural and Civil Engineering*, 15(1), pp. 227-243.
- [7] RakhshaniMehr, M., Esfahani, M. R., Kianoush M. R. (2014). Flexural ductility of reinforced concrete beams with lap-spliced bars, *Canadian Journal of Civil Engineering*, 41(7), pp. 594-604.
- [8] Ho, J., Kwan, A. and Pam, H. (2004). Minimum flexural ductility design of high-strength concrete beams, *Magazine of concrete research*, 56(1), pp. 13-22.
- [9] Zhang, J., Tao, X., Li, X., Zhang, Y., Liu, Y. (2022). Analytical and experimental investigation of the bond behavior of confined high-strength recycled aggregate concrete. *Construction and Building Materials*, 315, 125636.
- [10] Tamayo, J. L. P. and Garcia, G. O. (2021). Reassessment of the flexural behavior of high-strength reinforced concrete beams under short-term loads, *SN Applied Sciences*, 3(2), pp. 1-19.
- [11] Chowdhury, S. and Loo, Y. Cracking and damping in reinforced high strength concrete beams. pp. 749-754.
- [12] Ahmad, S. S. E., El-Shikh, M. Y. and Elmahdy, M. A. R. (2020). Effect of Confinement Techniques on Mechanical Behavior of Over-Reinforced HSC Beams, *MEJ. Mansoura Engineering Journal*, 42(4), pp. 21-26.
- [13] SikaWrap® Hex-230 C. SikaWrap® Hex-230 C Product Data Sheet. (2020).
https://doi.org/https://usa.sika.com/content/dam/dms/us01/g/sikawrap_hex-230c.pdf.
- [14] Sikadur®-330. Sikadur®-330 Product Data Sheet. (202=0).
- [15] ANSYS, (2019) ANSYS Release 19.0 Documentation.
- [16] Pereira, S.S.R., Carvalho, H., Dias, J. V. F., Mendes, V.R. V., Montenegro, P.A. (2019). Behavior of precast reinforced concrete columns subjected to monotonic short-term loading. *Frattura ed Integrità Strutturale*, 13(50), p. 242-250.
DOI: 10.3221/IGF-ESIS.50.20.
- [17] Sharaky, A., Torres, L. and Sallam, H. (2015). Experimental and analytical investigation into the flexural performance of RC beams with partially and fully bonded NSM FRP bars/strips, *Composite structures*, 122, pp. 113-126.